AMERICAN SOCIETY FOR MICROBIOLOGY | Applied and Environmental Microbiology®

GEOMICROBIOLOGY

Biomineralization of Cu_2S Nanoparticles by *Geobacter sulfurreducens*

Richard L. Kimber,[a] Heath Bagshaw,[a]* Kurt Smith,[a]* Dawn M. Buchanan,[a] Victoria S. Coker,[a] Jennifer S. Cavet,[b] Jonathan R. Lloyd[a]

[a]Williamson Research Centre for Molecular Environmental Science, Department of Earth and Environmental Sciences, University of Manchester, Manchester, United Kingdom

[b]School of Biological Sciences, Faculty of Biology Medicine and Health, University of Manchester, Manchester, United Kingdom

ABSTRACT Biomineralization of Cu has been shown to control contaminant dynamics and transport in soils. However, very little is known about the role that subsurface microorganisms may play in the biogeochemical cycling of Cu. In this study, we investigate the bioreduction of Cu(II) by the subsurface metal-reducing bacterium *Geobacter sulfurreducens*. Rapid removal of Cu from solution was observed in cell suspensions of *G. sulfurreducens* when Cu(II) was supplied, while transmission electron microscopy (TEM) analyses showed the formation of electron-dense nanoparticles associated with the cell surface. Energy-dispersive X-ray spectroscopy (EDX) point analysis and EDX spectrum image maps revealed that the nanoparticles are rich in both Cu and S. This finding was confirmed by X-ray absorption near-edge structure (XANES) and extended X-ray absorption fine structure (EXAFS) analyses, which identified the nanoparticles as Cu_2S. Biomineralization of Cu_xS nanoparticles in soils has been reported to enhance the colloidal transport of a number of contaminants, including Pb, Cd, and Hg. However, formation of these Cu_xS nanoparticles has only been observed under sulfate-reducing conditions and could not be repeated using isolates of implicated organisms. As *G. sulfurreducens* is unable to respire sulfate, and no reducible sulfur was supplied to the cells, these data suggest a novel mechanism for the biomineralization of Cu_2S under anoxic conditions. The implications of these findings for the biogeochemical cycling of Cu and other metals as well as the green production of Cu catalysts are discussed.

IMPORTANCE Dissimilatory metal-reducing bacteria are ubiquitous in soils and aquifers and are known to utilize a wide range of metals as terminal electron acceptors. These transformations play an important role in the biogeochemical cycling of metals in pristine and contaminated environments and can be harnessed for bioremediation and metal bioprocessing purposes. However, relatively little is known about their interactions with Cu. As a trace element that becomes toxic in excess, Cu can adversely affect soil biota and fertility. In addition, biomineralization of Cu nanoparticles has been reported to enhance the mobilization of other toxic metals. Here, we demonstrate that when supplied with acetate under anoxic conditions, the model metal-reducing bacterium *Geobacter sulfurreducens* can transform soluble Cu(II) to Cu_2S nanoparticles. This study provides new insights into Cu biomineralization by microorganisms and suggests that contaminant mobilization enhanced by Cu biomineralization could be facilitated by *Geobacter* species and related organisms.

KEYWORDS *Geobacter sulfurreducens*, copper, nanoparticles, Cu_2S, bioreduction

Dissimilatory metal-reducing bacteria are ubiquitous in soils and aquifers and are able to respire a wide range of metals coupled to the oxidation of organic or inorganic compounds (1, 2). These processes play an important role in the biogeo-

Citation Kimber RL, Bagshaw H, Smith K, Buchanan DM, Coker VS, Cavet JS, Lloyd JR. 2020. Biomineralization of Cu_2S nanoparticles by *Geobacter sulfurreducens*. Appl Environ Microbiol 86:e00967-20. https://doi.org/10.1128/AEM.00967-20.

Editor Hideaki Nojiri, University of Tokyo

Address correspondence to Richard L. Kimber, richard.kimber@manchester.ac.uk.

* Present address: Heath Bagshaw, Imaging Centre at Liverpool, University of Liverpool, Liverpool, United Kingdom; Kurt Smith, Chemical Sciences Division, Lawrence Berkeley National Laboratory, Berkeley, California, USA.

Received 27 April 2020
Accepted 10 July 2020
Accepted manuscript posted online 17 July 2020
Published 1 September 2020

chemical cycling of metals in soils and subsurface environments (3, 4). In addition, microbial metal reduction can be harnessed for catalytic applications (5, 6) and bioremediation purposes (7, 8). Species of *Geobacter* and *Shewanella* are among the most intensively studied metal reducers due to their presence in many soil and freshwater environments, their respiratory diversity, and the availability of genomic data (9–11). These organisms are able to utilize a range of metals as terminal electron acceptors, including Fe(III), Mn(IV), U(VI), Pu(VI), Cr(VI), Ag(I), Pd(II), and V(V) (3, 12–18). These processes typically involve *c*-type cytochromes, which facilitate electron transfer from the inner membrane to the periplasm and outer membrane, where many of these metals are reduced (19–21). Although the versatility of these metal reducers is well established, relatively little is known about their interactions with Cu.

Cu is a widely encountered trace element, with its distribution in soil affected by climate, geology, and soil properties (22). In addition, anthropogenic sources can lead to elevated Cu concentrations (23–26). Cu is an essential trace metal found in almost all forms of life; however, it can also be highly toxic by binding to proteins and inactivating enzyme function or by catalyzing Fenton chemistry to produce reactive oxygen species. Thus, at elevated concentrations, the inherent toxicity of Cu can limit plant growth, lowering crop yield and quality (27–29), and can decrease microbial community diversity and activity (30). Microbial processes play an important role in controlling the environmental fate of metals, potentially immobilizing them via redox changes, including bioreduction, or through sulfidation reactions (31). However, biomineralization has also been reported to enhance the mobilization of Cu and other cocontaminants through the formation of colloidal Cu nanoparticles (25, 32). For example, Hofacker et al. suggested *Clostridium* sp. was responsible for the Cu nanoparticle formation under soil reducing conditions; however, they were unable to directly observe Cu(II) reduction in cell suspensions of the *Clostridium* isolates (33). Therefore, further work is required to identify subsurface microorganisms which can potentially influence the biogeochemical behavior of this important micronutrient.

We demonstrated recently that *Shewanella oneidensis* is able to reductively precipitate Cu(0) nanoparticles from a Cu(II)-containing solution (6). Interestingly, the use of deletion mutants revealed that *c*-type cytochromes in the Mtr pathway, which is commonly used to reduce metals in *Shewanella* species, did not play a role in Cu(II) reduction. The as-prepared Cu nanoparticles were shown to be catalytically active toward a range of "click-chemistry" cycloaddition reactions, which have applications in the pharmaceutical industry (34).

Here, we investigate the fate of Cu(II) when supplied to cultures of another well-characterized model metal-reducing bacterium, the obligate anaerobe *Geobacter sulfurreducens*, in order to better understand its potential role in the biogeochemical cycling and the fate of Cu in contaminated soils and sediments, including the ability to produce Cu nanoparticles. Cu toxicity toward *G. sulfurreducens* was examined, and that bacterium's ability to bioreduce Cu(II) and remove the metal from solution was monitored using inductively coupled plasma atomic emission spectroscopy (ICP-AES). Any biomineralization products were analyzed using transmission electron microscopy (TEM), scanning transmission electron microscopy (STEM), energy-dispersive X-ray spectroscopy (EDX), X-ray absorption near-edge structure (XANES) analysis, and extended X-ray absorption fine structure (EXAFS) analysis.

RESULTS

Cu(II) toxicity toward *G. sulfurreducens*. The effect of a range of concentrations of Cu on the anaerobic growth of *G. sulfurreducens* in minimal medium with lactate and fumarate supplied as the electron donor and acceptor, respectively, is shown in Fig. 1. Supplementation of the medium with 100 nM or 1 μM Cu(II) had little or no effect on the growth of *G. sulfurreducens* relative to a control with no added Cu(II). However, supplementation with 10 μM Cu(II) caused an extended lag phase with little to no growth seen over the initial 24 hours and only 45% growth seen after 48 hours relative to the no added Cu(II) control. With 100 μM Cu(II) supplementation, no growth was

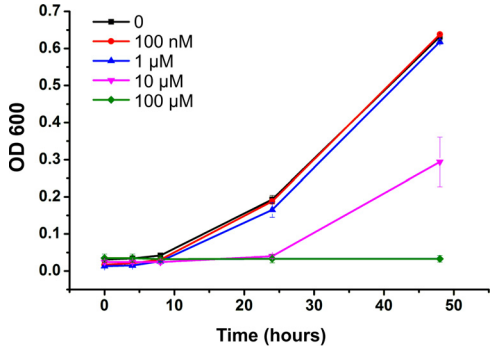

FIG 1 Anaerobic growth of *G. sulfurreducens* in minimal medium (NBAF) supplemented with different Cu(II) concentrations. Each concentration was performed in triplicate, with error bars representing the standard deviation of the replicates.

observed after 48 hours. Hence, under anoxic conditions, growth of *G. sulfurreducens* is strongly inhibited by Cu at concentrations of 10 μM and above.

Removal of Cu(II) and formation of Cu nanoparticles. Based on data from the toxicity assay and guided by Cu pore water concentrations in contaminated soils (25, 35), Cu(II) concentrations of 5 and 50 μM were chosen to be used in resting cell experiments to investigate the potential bioreduction of Cu(II) and the possible formation of lower oxidation state Cu nanoparticles, which was noted recently in cultures of other metal-reducing bacteria (6). Initial Cu(II) concentrations were confirmed via sampling of the solution prior to the addition of cells (t0). Decreases in the soluble Cu solution concentrations of 30.3% and 12.0% were observed in control experiments performed with dead (autoclaved) cells with initial concentrations of 5 μM and 50 μM Cu(II), respectively (Fig. 2). This decrease was observed at the first time point, taken immediately after inoculating the Cu(II)-containing medium with cells (t1), and then remained constant, consistent with initial Cu removal via rapid passive adsorption to the biomass. In the presence of live cells and an electron donor (acetate), a substantial further increase in Cu removal from solution compared with the dead (autoclaved) cell controls was observed, suggesting that most Cu removal in these treatments was facilitated by metabolic processes rather than by passive biosorption to the cell biomass (Fig. 2). When 5 μM Cu(II) was supplied, 50% Cu removal was observed

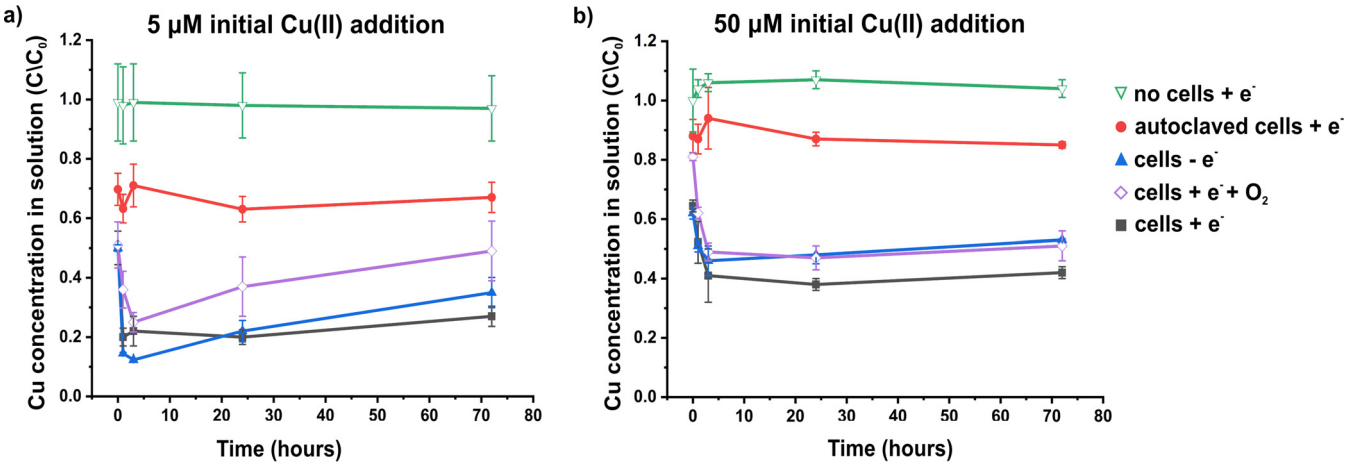

FIG 2 Concentration of Cu in solution in the presence of *G. sulfurreducens* when supplied with an initial Cu(II) concentration of 5 μM (a) or 50 μM (b). In both cases, Cu(II) was added to the medium prior to cell addition. The initial concentration of Cu was confirmed via ICP-AES. The first sampling time point (t1) was immediately after cell addition. Cu in solution was calculated as the concentration of Cu at a given time point (C) divided by the initial concentration prior to cell addition (C_0), as determined by ICP-AES. Experiments were performed under anoxic conditions, except where indicated with the addition of O_2 (purple diamonds). The addition or omission of acetate as an electron donor is indicated by $+e^-$ or $-e^-$, respectively. Each experiment was performed in triplicate, with error bars representing the standard deviation of these replicates.

immediately after addition of the cells (t1), with an increase to 80% removal at 1 hour. Cu removal remained stable at ~80% at 24 hours, with a small decrease to 73% seen at the final 72-hour time point. When an initial concentration of 50 μM Cu(II) was supplied, only 36% of the Cu was removed by the live cells at the first time point (t1). Removal of Cu continued slowly for up to 24 hours, reaching a maximum of 63% removal at 24 hours before decreasing again slightly to 58% removal at 72 hours. Oxygenated cell controls (with acetate) showed decreased Cu removal at all time points compared with the anoxic cells when challenged with either 5 μM or 50 μM Cu(II). When no electron donor was supplied, initial Cu removal was slightly enhanced relative to the acetate-amended system when challenged with 5 μM Cu(II). However, after 3 h, Cu solution concentrations remained relatively stable in the acetate-amended experiment, but a significant increase in Cu solution concentrations was observed in both the electron donor-free and oxygenated cell controls. When the final sample was taken at 72 hours, Cu removal was greatest in the anoxic cells supplied with acetate for both the 5 μM and 50 μM Cu(II)-challenged systems.

TEM images of samples taken at 24 hours demonstrated that when bacteria were supplied with acetate as an electron donor under anoxic conditions, removal of Cu by *G. sulfurreducens* resulted in the biomineralization of Cu nanoparticles (Fig. 3). These Cu nanoparticles were typically spherical and predominately associated with the cells, ranging in size from 10 to 90 nm.

EDX point analysis indicated that the particles were both Cu and S rich (Fig. 3). This finding was further supported by EDX spectrum imaging performed during STEM that revealed a close association between Cu and S in the nanoparticles (Fig. 4). A few particles were also seen in the dead (autoclaved) control; however, they were typically larger (100 to 200 nm) agglomerates and were far fewer than with live cells supplied with acetate. EDX analysis indicated these particles were also Cu and S rich (see Fig. S1 in the supplemental material). No nanoparticles were observed in the oxygenated cell control or no electron donor control (see Fig. S2 in the supplemental material).

XAS characterization. To identify the speciation of Cu and the local valence structure of the metallic nanoparticles, XAS characterization was performed on beamline B18 at the Diamond Light Source. The Cu K-edge X-ray absorption near-edge structure (XANES) spectrum collected on the Cu nanoparticles precipitated by *G. sulfurreducens* had an absorption edge energy (E_0) of 8,980.4 eV. This aligned well with the E_0 energy of a Cu_2S (chalcocite) standard (8,980.1 eV). The excellent match between the XANES spectra for the Cu nanoparticles and the Cu_2S standard clearly demonstrates that washed cell suspensions of the metal-reducing bacterium *G. sulfurreducens* catalyzed the formation of Cu_2S particles (Fig. 5a). The oxidation state of Cu in Cu_2S is thought to be dominated by Cu(I); however, the presence of significant Cu(II) and Cu(0) has also been suggested (36, 37). XANES data were identical whether the Cu nanoparticles were formed when the cells were supplied with Cu(II) as $CuSO_4$ or $CuCl_2$, ruling out any impact from the salt (data not shown).

Given the similarity between the Cu nanoparticles and Cu_2S XANES spectra, the Cu nanoparticle EXAFS data were fitted assuming a coordination environment similar to that of the mineral chalcocite (Cu_2S) (38). The best fit (Fig. 5b) was obtained with one shell of 3 S atoms at 2.30 $\pm$ 0.01 Å with a Debye-Waller factor of 0.009 $\pm$ 0.001. This is consistent with a Cu_2S-like structure where Cu is coordinated by 3 S atoms at approximately 2.3 Å. Cu_2S has 6 Cu atoms in the second shell; however, the Cu-S interatomic distance is poorly constrained (2.60 to 3.30 Å) and is likely to reduce the contribution from Cu scatterers to the EXAFS spectrum. Given this, the EXAFS data do not preclude the formation of a Cu_2S phase. See Table S1 in the supplemental material for a complete description of the EXAFS fitting. Collectively, the XANES and EXAFS data support the biomineralization of the Cu(II) as poorly ordered Cu_2S.

Cu $L_{2,3}$-edge XAS was also performed on selected samples at the Advanced Light Source, Berkeley, CA. When live cells were supplied with an electron donor, peaks at 930.7 and 933.4 eV were observed (see Fig. S3 in the supplemental material). The peak

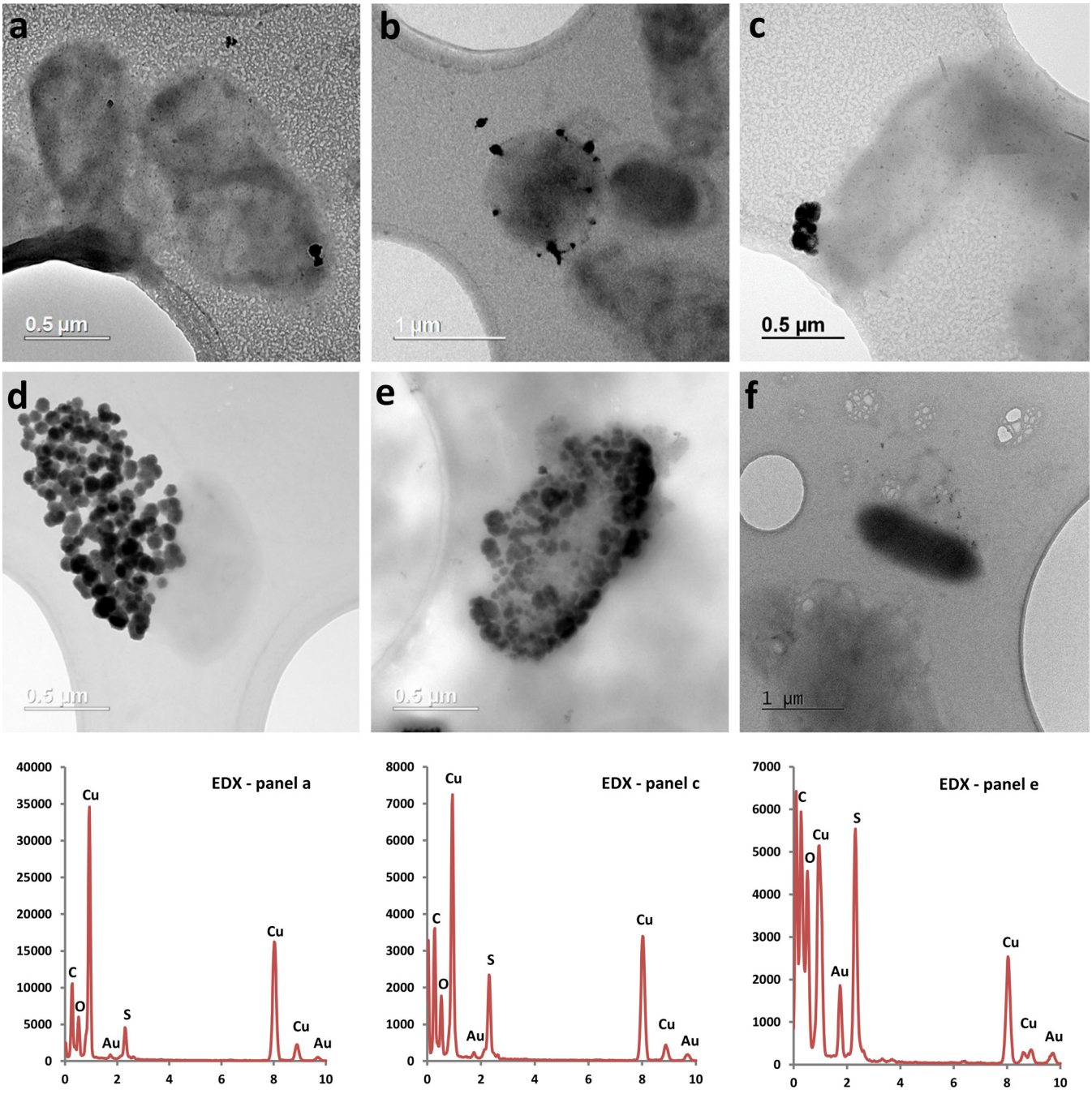

FIG 3 TEM images of *G. sulfurreducens* with associated Cu nanoparticles after being supplied with 5 μM Cu(II) (a to c) and 50 μM Cu(II) (d to f). The bottom row shows the corresponding EDX spectra of particles from panels a, c, and e (left to right). The *x* axis displays energy (keV), with the *y* axis displaying total counts. Samples for TEM imaging were taken at 24 h.

at 930.7 eV is indicative of Cu(II), whereas the peak at 933.4 eV reflects the presence of Cu(I) (39, 40). Although the peak at 930.7 eV is qualitatively larger than the peak at 933.4 eV, the Cu(II) is known to be approximately 25 times more intense than the Cu(I) peak (39), suggesting a significant presence of Cu(I) in the sample and confirming that bioreduction took place. Cu $L_{2,3}$-edge XAS data from the autoclaved and no electron donor controls also display peaks indicative of Cu(II) and Cu(I), although with a noticeable shift of +0.3 eV in peak positions. The intensities of the Cu(I) peaks are qualitatively smaller in both controls than in the live cells supplied with an electron donor, suggesting that less Cu bioreduction occurred in the controls.

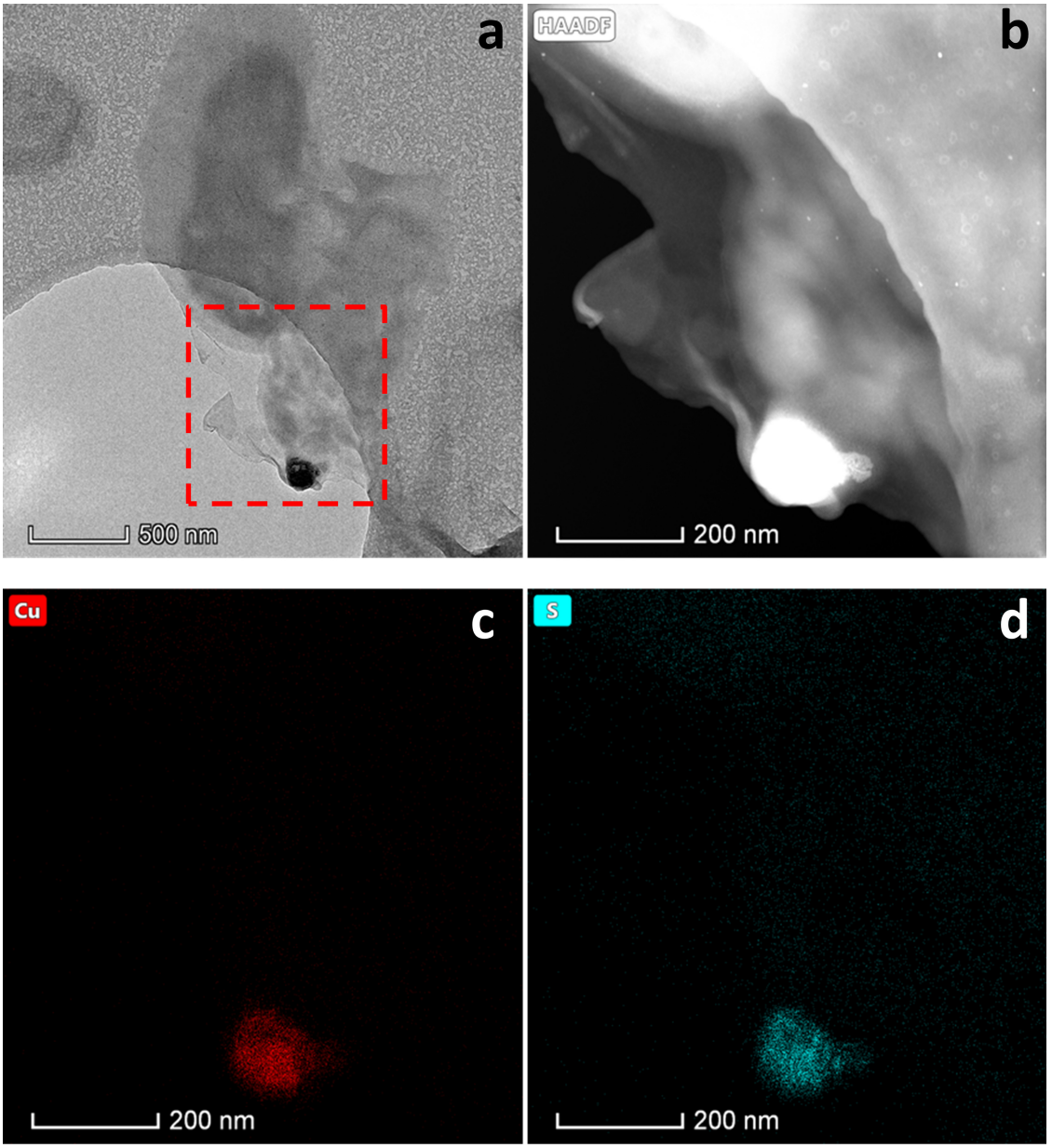

FIG 4 (a) TEM image of cells with Cu nanoparticles. (b) High-angle annular dark field (HAADF) image of the red dashed square from panel a. (c and d) EDX spectrum imaging of panel b, taken under STEM, showing Cu (c) and S (d).

DISCUSSION

Cu toxicity toward *G. sulfurreducens*. Our results demonstrate that under anoxic conditions, concentrations as low as 10 μM Cu(II) strongly inhibit the growth of *G. sulfurreducens*. This value is over an order of magnitude lower than the Cu(II) concentrations (>100 μM) that are reported to be required to inhibit the growth of the enteric model organism *Escherichia coli* under similar conditions (anoxic chemically defined medium) (39). In a recent study, the model Fe(III)-reducing bacterium *Shewanella oneidensis* also appears to have greater resistance to Cu toxicity than *G. sulfurreducens*, with some growth of *S. oneidensis* still observed at 100 μM Cu in a similar chemically defined medium (6, 40), whereas growth of *G. sulfurreducens* is inhibited completely (Fig. 1). Hence, *G. sulfurreducens* appears to be particularly vulnerable to Cu toxicity.

Biomineralization of Cu nanoparticles. The relatively low tolerance of *G. sulfurreducens* toward Cu(II) compared with *S. oneidensis* is also reflected in their respective

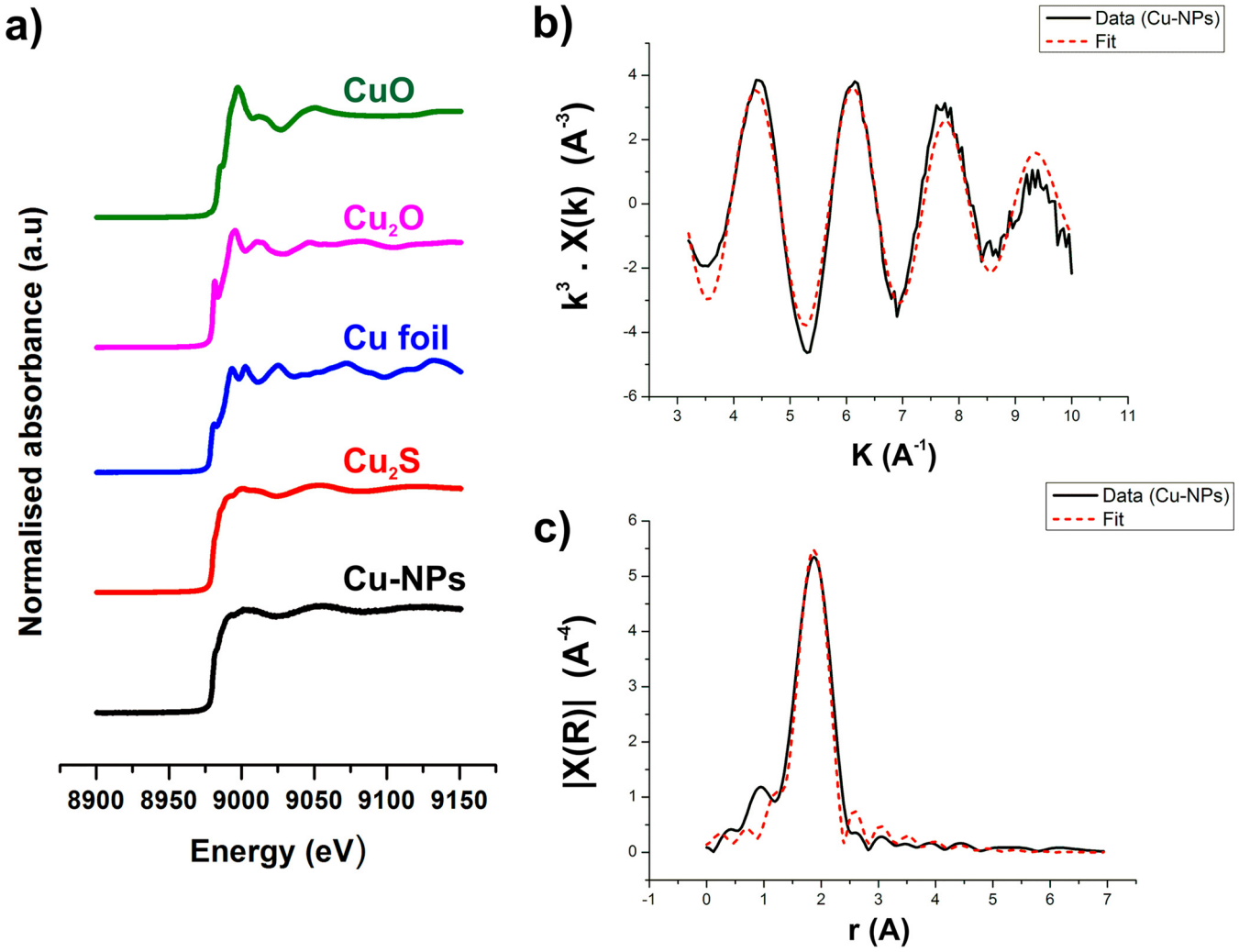

FIG 5 (a) XANES for the Cu K-edge of Cu nanoparticles produced by *G. sulfurreducens* (black line) and Cu standards. K^3-weighted EXAFS data (b) and corresponding Fourier transform (c) for the Cu K-edge of the Cu nanoparticles (Cu-NPs). Data are shown by the black (solid) line, and the fit is shown by the red (dotted) line.

abilities to reduce Cu(II). In our previous study, a complete reduction of 50 μM and partial reduction of up to 200 μM Cu(II) to Cu(0) was observed for *S. oneidensis* (6). In the present study, *G. sulfurreducens* was capable of removing only up to 80% and 63% of 5 μM and 50 μM Cu(II) from solution, respectively. No removal at 200 μM Cu(II) was observed (data not shown). Our data suggest that Cu removal from solution is greatest in the presence of live cells, suggesting that microbial metabolism increases the removal of Cu from solution compared with biosorption by dead biomass. The highest removal was seen when live cells were supplied with an electron donor under anoxic conditions, with TEM and XAS data indicating that formation of Cu nanoparticles was significant only under these conditions. This result suggests that the presence of an electron donor and anoxic conditions are required for significant biosynthesis of Cu nanoparticles. Our characterization of these nanoparticles as Cu_2S is supported by EDX point analysis, EDX mapping, XANES, and EXAFS data. As no nanoparticles were seen in the oxygenated or electron donor-free controls and XAS data support limited reduction to Cu(I) species, we attribute the observed removal of Cu from solution under these conditions to biosorption of Cu(II) to the cell surface and/or intracellular accumulation of the metal. Interestingly, the Cu solution concentrations in the oxygenated and electron donor-free controls were found to increase after 3 hours, but they remained relatively stable under anoxic conditions with an electron donor (acetate). We

suggest that the rerelease of Cu into solution observed in the oxygenated and electron donor-free controls may be due to the export of intracellular Cu and/or desorption of cell-bound Cu, which was limited in the anoxic cells supplied with acetate due to immobilization of Cu via bioreduction and Cu_2S precipitation.

The formation of Cu_2S nanoparticles here is surprising, as previous work on Cu biomineralization by anaerobic bacteria found that, in the absence of sulfate-reducing conditions, nanoparticles formed were metallic Cu or Cu oxides (6, 25, 41, 42). Several mechanisms have been proposed for the formation of Cu(0) nanoparticles among different bacteria. Ramanathan et al. suggested that intracellular reduction and cellular efflux systems may play a role in the synthesis of extracellular Cu(0) nanoparticles by *Morganella morganii* (42). *Clostridium* species were implicated in the formation of Cu(0) nanoparticles in a flooded Cu-contaminated soil via cellular efflux of Cu(I), followed by disproportionation to Cu(II) and Cu(0) (25, 33). Conversion of the Cu(0) nanoparticles to Cu_xS in the flooded soil was observed following the onset of sulfate reduction. As *G. sulfurreducens* is unable to carry out dissimilatory sulfate reduction, this mechanism cannot account for the formation of Cu_2S nanoparticles seen here. Identical XANES spectra from Cu nanoparticles formed when *G. sulfurreducens* was supplied with Cu(II) as $CuSO_4$ or $CuCl_2$, further supporting a mechanism which does not directly involve sulfate reduction. Clearly, a different mechanism is responsible for the biomineralization of Cu_2S nanoparticles in *G. sulfurreducens* than that for the Cu(0) nanoparticles typically produced by other bacteria studied to date.

Cell-bound thiol sites have been shown to dominate metal(oid) complexation in a range of microorganisms, including *G. sulfurreducens* (43, 44). In addition, intracellular Cu(I) is known to target Fe-S clusters in *Escherichia coli* under anoxic conditions, with Cu(I) displacing the Fe (45–47). Ligation of Cu with these sulfur groups could potentially play a role in the formation of Cu_xS nanoparticles in organisms which are unable to reduce Cu(II) to Cu(0), such as *G. sulfurreducens*. However, elucidating the mechanisms of Cu nanoparticle formation in metal-reducing bacteria requires further work and will be the target of future studies.

This study demonstrates that *G. sulfurreducens*, a metal-reducing bacterium, is able to produce Cu_2S nanoparticles from aqueous Cu(II). These results provide direct evidence of Cu biomineralization by a ubiquitous subsurface microorganism, which may suggest a role for this organism in the biogeochemical cycling of Cu and potential mobilization of cocontaminants in soil systems (25). Cu_xS nanoparticles have previously been reported to form only following the onset of sulfate reduction. *G. sulfurreducens* is unable to respire sulfate, suggesting that biomineralization of Cu_xS nanoparticles could also occur in the absence of sulfate-reducing conditions. In addition to the biogeochemical implications discussed above, biomineralization of Cu nanoparticles offers a promising green method for the production of Cu catalysts. We have previously demonstrated that Cu(0) nanoparticles produced by *S. oneidensis* are active click-chemistry catalysts (6). Cu_2S nanoparticles also have many catalytic applications, including as electrocatalysts for oxygen evolution and CO_2 reduction (48, 49). Therefore, tailored Cu nanoparticle catalysts could potentially be produced using specific microorganisms.

MATERIALS AND METHODS

Geobacter sulfurreducens. All cultures of *G. sulfurreducens* (ATCC 51573) were grown anaerobically in a fully defined, presterilized, liquid minimal medium (NBAF) (50) at pH 7.1. Serum bottles (100 ml) containing NBAF were inoculated with a late-log/early-stationary-phase culture to give an optical density at 600 nm (OD_{600}) of 0.02. The cultures were grown for 24 h at 30°C. Late-log cultures were transferred under anoxic conditions to centrifuge tubes, and the cells were pelleted by centrifugation at 4,960 rpm for 20 min at 4°C. The cells were washed two times with fresh anoxic, sterilized morpholinepropanesulfonic acid (MOPS) buffer (50 mM) and then were resuspended in the same buffer at pH 7.1.

Toxicity assay. Cells were grown in minimal medium as described above. Late-log-phase aliquots were used to inoculate 50 ml of anoxic minimal medium to give a starting OD_{600} of 0.015. Cu ($CuSO_4$) was added from a stock solution to give a final concentration of 1 nM or 0.1, 1, 10, or 100 μM Cu(II). A Cu-free control was also used. Incubation was carried out at 30°C. Samples were taken under anoxic, aseptic conditions at 0, 4, 8, 24, and 48 h, and the optical density was measured to determine growth. All assays were performed in triplicate with a standard deviation of less than 0.012 between OD_{600} readings.

Cu removal experiments. The removal of Cu(II) by *G. sulfurreducens* was determined using pregrown and washed "resting cell" cultures supplied with excess electron donor. The cultures contained either 5 μM or 50 μM Cu(II) as $CuSO_4$ (unless stated otherwise) and 30 mM sodium acetate as the electron donor in 50 mM MOPS adjusted to pH 7.1. The medium was purged with a gas mixture of N_2:CO_2 (80:20) for 20 minutes to remove O_2, sealed in containers with thick butyl rubber stoppers, and autoclaved. Washed late-log/early-stationary-phase cells were then added aseptically to achieve a final OD_{600} of 0.2, and incubation was carried out at 30°C. Soluble Cu was determined by taking aliquots and centrifuging them at 14,900 $\times$ *g* for 10 minutes to pellet the cells and insoluble Cu. Samples were taken from the supernatant and Cu in solution measured using ICP-AES. All experiments were performed in triplicate.

TEM imaging. All sample preparations were performed under anoxic conditions in an anaerobic cabinet. A total of 1 ml of cell suspension from the Cu reduction assay (5 and 50 μM) was taken after 24 hours and centrifuged at 14,900 $\times$ *g* for 10 minutes; afterward, the supernatant was discarded and the pellet resuspended in 1 ml deionized water. A total of 1.5 μl of the cell suspension was pipetted onto a gold TEM grid with a carbon-coated Formvar or holey-carbon support film and air dried in an anaerobic chamber. Samples were kept anoxic until they were transferred into the TEM chamber. TEM imaging and EDX analysis were performed in an FEI TF 30 field emission gun (FEG) analytical TEM operated at 300 kV and equipped with an Oxford X-Max 80 windowless silicon drift detector (SSD) EDS system. EDX analysis was performed with the sample tilted at the optimum angle toward the detector to increase collection efficiency.

STEM imaging. STEM imaging and EDX analysis were performed in an FEI Talos F200A analytical transmission electron microscope (AEM) with an X-FEG electron source operated at 200 kV. High-angle annular dark field (HAADF) STEM imaging was performed using a probe current of approximately 250 pA. EDX analysis was performed using a Super-X four silicon drift detector EDX system with a total collection solid angle of 0.7 srad; all four detectors were turned on, and the sample was not tilted.

XAS characterization. For XAS characterization at the Cu K-edge, 1-ml aliquots of the *G. sulfurreducens* Cu reduction (5 and 50 μM $CuSO_4$ and $CuCl_2$) assays were taken and centrifuged at 14,900 $\times$ *g* for 10 minutes. The supernatant was discarded and the pellet resuspended in 1 ml anoxic deionized water. The sample was centrifuged again and resuspended in 1 ml anoxic deionized water before 200 μl of the suspension was pipetted onto a plastic weighing boat and air dried. Samples were mounted onto a layer of Kapton tape which in turn was mounted onto an aluminum sample holder. A further layer of Kapton tape was applied over the samples to maintain anaerobicity. X-ray absorption fine structure (XAFS) spectra were collected at the Cu K-edge (~8,980 eV) at room temperature on beamline B18 at the Diamond Light Source. A 36-element solid-state Ge detector with digital signal processing for fluorescence XAFS, high-energy resolution, and high count rate was used to measure with the beam at 45° incidence with respect to the sample holder plane. All spectra were acquired in quick-EXAFS mode, using the Pt-coated branch of collimating and focusing mirrors, an Si(111) double-crystal monochromator, and a pair of harmonic rejection mirrors.

XAS processing and background subtraction were carried out using Athena, whereas EXAFS data were modeled using Artemis (Demeter 0.9.24 [51]). Fitting was calculated using multiple k-weights (k, k^2, and k^3) and the best fit was calculated in R space by minimization of the reduced χ^2. At no point did the parameterization utilize more than two-thirds of the independent points available.

Cu $L_{2/3}$-edge spectroscopy was performed at the Advanced Light Source, Berkeley, CA, on beamline 6.3.1.1. For sample preparation, 1-ml aliquots were taken and centrifuged at 14,900 $\times$ *g* for 10 min. The supernatant was discarded and the pellet resuspended in 1 ml anoxic deionized water. The sample was centrifuged again before final resuspension in 1 ml anoxic deionized water. A total of 200 μl of the suspension was dried as a powder onto a carbon sticky pad before being placed on an aluminum sample holder and stored under anoxic conditions prior to analysis. All manipulations were performed in an anaerobic chamber. X-ray absorption spectra were collected in total-electron yield (TEY) mode and normalized to the incident beam intensity.

SUPPLEMENTAL MATERIAL

Supplemental material is available online only.

SUPPLEMENTAL FILE 1, PDF file, 1.2 MB.

ACKNOWLEDGMENTS

We thank NERC for funding under the Resource Recovery from Waste program (NE/L014203/1) and acknowledge support from the BBSRC (grants BB/L013711/1 and BB/R010412/1). K.S. acknowledges EnvRadNet and ST/K001787/1 for funding. We acknowledge beamtime awarded at the Diamond Light Source for XANES and EXAFS on beamline B18 under proposals SP-13705 and SP-16136. This research used resources of the Advanced Light Source, a DOE Office of Science User Facility under contract no. DE-AC02-05CH11231.

We also thank P. Lythgoe (University of Manchester) for ICP-AES analysis. We thank Giannantonio Cibin for his assistance on B18.

REFERENCES

1. Lovley DR, Phillips E. 1988. Novel mode of microbial energy metabolism: organic carbon oxidation coupled to dissimilatory reduction of iron or manganese. Appl Environ Microbiol 54:1472–1480. https://doi.org/10.1128/AEM.54.6.1472-1480.1988.
2. Lovley DR. 1993. Dissimilatory metal reduction. Annu Rev Microbiol 47:263–290. https://doi.org/10.1146/annurev.mi.47.100193.001403.
3. Lovley DR, Holmes DE, Nevin KP. 2004. Dissimilatory Fe(III) and Mn(IV) reduction. Adv Microb Physiol 49:219–286. https://doi.org/10.1016/S0065-2911(04)49005-5.
4. Williamson AJ, Morris K, Shaw S, Byrne JM, Boothman C, Lloyd JR. 2013. Microbial reduction of Fe(III) under alkaline conditions relevant to geological disposal. Appl Environ Microbiol 79:3320–3326. https://doi.org/10.1128/AEM.03063-12.
5. Søbjerg LS, Gauthier D, Lindhardt AT, Bunge M, Finster K, Meyer RL, Skrydstrup T. 2009. Bio-supported palladium nanoparticles as a catalyst for Suzuki–Miyaura and Mizoroki–Heck reactions. Green Chem 11:2041–2046. https://doi.org/10.1039/b918351p.
6. Kimber RL, Lewis EA, Parmeggiani F, Smith K, Bagshaw H, Starborg T, Joshi N, Figueroa AI, van der Laan G, Cibin G, Gianolio D, Haigh SJ, Pattrick RAD, Turner NJ, Lloyd JR. 2018. Biosynthesis and characterization of copper nanoparticles using *Shewanella oneidensis*: application for click chemistry. Small 14:1703145. https://doi.org/10.1002/smll.201703145.
7. Lloyd JR. 2003. Microbial reduction of metals and radionuclides. FEMS Microbiol Rev 27:411–425. https://doi.org/10.1016/S0168-6445(03)00044-5.
8. Gadd GM. 2010. Metals, minerals and microbes: geomicrobiology and bioremediation. Microbiology 156:609–643. https://doi.org/10.1099/mic.0.037143-0.
9. Methé BA, Nelson KE, Eisen JA, Paulsen IT, Nelson W, Heidelberg JF, Wu D, Wu M, Ward N, Beanan MJ, Dodson RJ, Madupu R, Brinkac LM, Daugherty SC, DeBoy RT, Durkin AS, Gwinn M, Kolonay JF, Sullivan SA, Haft DH, Selengut J, Davidsen TM, Zafar N, White O, Tran B, Romero C, Forberger HA, Weidman J, Khouri H, Feldblyum TV, Utterback TR, Van Aken SE, Lovley DR, Fraser CM. 2003. Genome of *Geobacter sulfurreducens*: metal reduction in subsurface environments. Science 302:1967–1969. https://doi.org/10.1126/science.1088727.
10. Heidelberg JF, Paulsen IT, Nelson KE, Gaidos EJ, Nelson WC, Read TD, Eisen JA, Seshadri R, Ward N, Methe B, Clayton RA, Meyer T, Tsapin A, Scott J, Beanan M, Brinkac L, Daugherty S, DeBoy RT, Dodson RJ, Durkin AS, Haft DH, Kolonay JF, Madupu R, Peterson JD, Umayam LA, White O, Wolf AM, Vamathevan J, Weidman J, Impraim M, Lee K, Berry K, Lee C, Mueller J, Khouri H, Gill J, Utterback TR, McDonald LA, Feldblyum TV, Smith HO, Venter C, Nealson KH, Fraser CM. 2002. Genome sequence of the dissimilatory metal ion–reducing bacterium *Shewanella oneidensis*. Nat Biotechnol 20:1118–1123. https://doi.org/10.1038/nbt749.
11. Fredrickson JK, Romine MF. 2005. Genome-assisted analysis of dissimilatory metal-reducing bacteria. Curr Opin Biotechnol 16:269–274. https://doi.org/10.1016/j.copbio.2005.04.001.
12. Marshall MJ, Beliaev AS, Dohnalkova AC, Kennedy DW, Shi L, Wang Z, Boyanov MI, Lai B, Kemner KM, McLean JS, Reed SB, Culley DE, Bailey VL, Simonson CJ, Saffarini DA, Romine MF, Zachara JM, Fredrickson JK. 2006. *c*-Type cytochrome-dependent formation of U(IV) nanoparticles by *Shewanella oneidensis*. PLoS Biol 4:e268. https://doi.org/10.1371/journal.pbio.0040268.
13. Icopini GA, Lack JG, Hersman LE, Neu MP, Boukhalfa H. 2009. Plutonium(V/VI) reduction by the metal-reducing bacteria *Geobacter metallireducens* GS-15 and *Shewanella oneidensis* MR-1. Appl Environ Microbiol 75:3641–3647. https://doi.org/10.1128/AEM.00022-09.
14. Liu C, Gorby YA, Zachara JM, Fredrickson JK, Brown CF. 2002. Reduction kinetics of Fe(III), Co(III), U(VI), Cr(VI), and Tc(VII) in cultures of dissimilatory metal-reducing bacteria. Biotechnol Bioeng 80:637–649. https://doi.org/10.1002/bit.10430.
15. Belchik SM, Kennedy DW, Dohnalkova AC, Wang Y, Sevinc PC, Wu H, Lin Y, Lu HP, Fredrickson JK, Shi L. 2011. Extracellular reduction of hexavalent chromium by cytochromes MtrC and OmcA of *Shewanella oneidensis* MR-1. Appl Environ Microbiol 77:4035–4041. https://doi.org/10.1128/AEM.02463-10.
16. Law N, Ansari S, Livens FR, Renshaw JC, Lloyd JR. 2008. Formation of nanoscale elemental silver particles via enzymatic reduction by *Geobacter sulfurreducens*. Appl Environ Microbiol 74:7090–7093. https://doi.org/10.1128/AEM.01069-08.
17. Ng CK, Cai Tan TK, Song H, Cao B. 2013. Reductive formation of palladium nanoparticles by *Shewanella oneidensis*: role of outer membrane cytochromes and hydrogenases. RSC Adv 3:22498–22503. https://doi.org/10.1039/c3ra44143a.
18. Carpentier W, Sandra K, De Smet I, Brigé A, De Smet L, Van Beeumen J. 2003. Microbial reduction and precipitation of vanadium by *Shewanella oneidensis*. Appl Environ Microbiol 69:3636–3639. https://doi.org/10.1128/aem.69.6.3636-3639.2003.
19. Shi L, Squier TC, Zachara JM, Fredrickson JK. 2007. Respiration of metal (hydr)oxides by *Shewanella* and *Geobacter*: a key role for multihaem c-type cytochromes. Mol Microbiol 65:12–20. https://doi.org/10.1111/j.1365-2958.2007.05783.x.
20. Ueki T, DiDonato LN, Lovley DR. 2017. Toward establishing minimum requirements for extracellular electron transfer in *Geobacter sulfurreducens*. FEMS Microbiol Lett 364:10.1093/femsle/fnx093. https://doi.org/10.1093/femsle/fnx093.
21. Levar CE, Hoffman CL, Dunshee AJ, Toner BM, Bond DR. 2017. Redox potential as a master variable controlling pathways of metal reduction by *Geobacter sulfurreducens*. ISME J 11:741–752. https://doi.org/10.1038/ismej.2016.146.
22. Ballabio C, Panagos P, Lugato E, Huang J-H, Orgiazzi A, Jones A, Fernandez-Ugalde O, Borrelli P, Montanarella L. 2018. Copper distribution in European topsoils: an assessment based on LUCAS soil survey. Sci Total Environ 636:282–298. https://doi.org/10.1016/j.scitotenv.2018.04.268.
23. Pietrzak U, McPhail DC. 2004. Copper accumulation, distribution and fractionation in vineyard soils of Victoria, Australia. Geoderma 122:151–166. https://doi.org/10.1016/j.geoderma.2004.01.005.
24. Turpeinen R, Kairesalo T, Häggblom MM. 2004. Microbial community structure and activity in arsenic-, chromium- and copper-contaminated soils. FEMS Microbiol Ecol 47:39–50. https://doi.org/10.1016/S0168-6496(03)00232-0.
25. Weber F-A, Voegelin A, Kaegi R, Kretzschmar R. 2009. Contaminant mobilization by metallic copper and metal sulphide colloids in flooded soil. Nat Geosci 2:267–271. https://doi.org/10.1038/ngeo476.
26. Balasoiu CF, Zagury GJ, Deschênes L. 2001. Partitioning and speciation of chromium, copper, and arsenic in CCA-contaminated soils: influence of soil composition. Sci Total Environ 280:239–255. https://doi.org/10.1016/s0048-9697(01)00833-6.
27. Mocquot B, Vangronsveld J, Clijsters H, Mench M. 1996. Copper toxicity in young maize (Zea mays L.) plants: effects on growth, mineral and chlorophyll contents, and enzyme activities. Plant Soil 182:287–300. https://doi.org/10.1007/BF00029060.
28. Maksymiec W. 1998. Effect of copper on cellular processes in higher plants. Photosynthetica 34:321–342. https://doi.org/10.1023/A:1006818815528.
29. Yruela I. 2005. Copper in plants. Braz J Plant Physiol 17:145–156. https://doi.org/10.1590/S1677-04202005000100012.
30. Smit E, Leeflang P, Wernars K. 2006. Detection of shifts in microbial community structure and diversity in soil caused by copper contamination using amplified ribosomal DNA restriction analysis. FEMS Microbiol Ecol 23:249–261. https://doi.org/10.1111/j.1574-6941.1997.tb00407.x.
31. Anderson RT, Vrionis HA, Ortiz-Bernad I, Resch CT, Long PE, Dayvault R, Karp K, Marutzky S, Metzler DR, Peacock A, White DC, Lowe M, Lovley DR. 2003. Stimulating the in situ activity of Geobacter species to remove uranium from the groundwater of a uranium-contaminated aquifer. Appl Environ Microbiol 69:5884–5891. https://doi.org/10.1128/aem.69.10.5884-5891.2003.
32. Hofacker AF, Voegelin A, Kaegi R, Kretzschmar R. 2013. Mercury mobilization in a flooded soil by incorporation into metallic copper and metal sulfide nanoparticles. Environ Sci Technol 47:7739–7746. https://doi.org/10.1021/es4010976.
33. Hofacker AF, Behrens S, Voegelin A, Kaegi R, Lösekann-Behrens T, Kappler A, Kretzschmar R. 2015. *Clostridium* species as metallic copper-forming bacteria in soil under reducing conditions. Geomicrobiol J 32:130–139. https://doi.org/10.1080/01490451.2014.933287.
34. Kolb HC, Sharpless KB. 2003. The growing impact of click chemistry on drug discovery. Drug Discov Today 8:1128–1137. https://doi.org/10.1016/s1359-6446(03)02933-7.
35. Vulkan R, Zhao F-J, Barbosa-Jefferson V, Preston S, Paton GI, Tipping E, McGrath SP. 2000. Copper speciation and impacts on bacterial biosensors in the pore water of copper-contaminated soils. Environ Sci Technol 34:5115–5121. https://doi.org/10.1021/es0000910.

36. Gupta S, Chandna N, Singh AK, Jain N. 2018. Regioselective synthesis of N^2-alkylated-1,2,3 triazoles and N^1-alkylated benzotriazoles: Cu_2S as a recyclable nanocatalyst for oxidative amination of N,N-dimethylbenzylamines. J Org Chem 83:3226–3235. https://doi.org/10.1021/acs.joc.8b00107.
37. Kumar P, Nagarajan R, Sarangi R. 2013. Quantitative X-ray absorption and emission spectroscopies: electronic structure elucidation of Cu_2S and CuS. J Mater Chem C 1:2448–2454. https://doi.org/10.1039/C3TC00639E.
38. Evans HT. 1971. Crystal structure of low chalcocite. Nat Phys 232:69–70. https://doi.org/10.1038/physci232069a0.
39. Outten FW, Huffman DL, Hale JA, O'Halloran TV. 2001. The independent cue and cus systems confer copper tolerance during aerobic and anaerobic growth in *Escherichia coli*. J Biol Chem 276:30670–30677. https://doi.org/10.1074/jbc.M104122200.
40. Toes ACM, Geelhoed JS, Kuenen JG, Muyzer G. 2008. Characterization of heavy metal resistance of metal-reducing *Shewanella* isolates from marine sediments. Geomicrobiol J 25:304–314. https://doi.org/10.1080/01490450802258329.
41. Singh AV, Patil R, Anand A, Milani P, Gade W. 2010. Biological synthesis of copper oxide nano particles using *Escherichia coli*. Curr Nanosci 6:365–369. https://doi.org/10.2174/157341310791659062.
42. Ramanathan R, Field MR, O'Mullane AP, Smooker PM, Bhargava SK, Bansal V. 2013. Aqueous phase synthesis of copper nanoparticles: a link between heavy metal resistance and nanoparticle synthesis ability in bacterial systems. Nanoscale 5:2300–2306. https://doi.org/10.1039/c2nr32887a.
43. Mishra B, Shoenfelt E, Yu Q, Yee N, Fein JB, Myneni S. 2017. Stoichiometry of mercury-thiol complexes on bacterial cell envelopes. Chem Geol 464:137–146. https://doi.org/10.1016/j.chemgeo.2017.02.015.
44. Mishra B, Boyanov M, Bunker BA, Kelly SD, Kemner KM, Fein JB. 2010. High- and low-affinity binding sites for Cd on the bacterial cell walls of *Bacillus subtilis* and *Shewanella oneidensis*. Geochim Cosmochim Acta 74:4219–4233. https://doi.org/10.1016/j.gca.2010.02.019.
45. Macomber L, Imlay JA. 2009. The iron-sulfur clusters of dehydratases are primary intracellular targets of copper toxicity. Proc Natl Acad Sci U S A 106:8344–8349. https://doi.org/10.1073/pnas.0812808106.
46. Tan G, Yang J, Li T, Zhao J, Sun S, Li X, Lin C, Li J, Zhou H, Lyu J, Ding H. 2017. Anaerobic copper toxicity and iron-sulfur cluster biogenesis in *Escherichia coli*. Appl Environ Microbiol 83:e00867-17. https://doi.org/10.1128/AEM.00867-17.
47. Tan G, Cheng Z, Pang Y, Landry AP, Li J, Lu J, Ding H. 2014. Copper binding in IscA inhibits iron-sulphur cluster assembly in *Escherichia coli*. Mol Microbiol 93:629–644. https://doi.org/10.1111/mmi.12676.
48. Coughlan C, Ibáñez M, Dobrozhan O, Singh A, Cabot A, Ryan KM. 2017. Compound copper chalcogenide nanocrystals. Chem Rev 117:5865–6109. https://doi.org/10.1021/acs.chemrev.6b00376.
49. An L, Zhou P, Yin J, Liu H, Chen F, Liu H, Du Y, Xi P. 2015. Phase transformation fabrication of a Cu_2S nanoplate as an efficient catalyst for water oxidation with glycine. Inorg Chem 54:3281–3289. https://doi.org/10.1021/ic502920r.
50. Muhamadali H, Xu Y, Ellis DI, Allwood JW, Rattray NJW, Correa E, Alrabiah H, Lloyd JR, Goodacre R. 2015. Metabolic profiling of *Geobacter sulfurreducens* during industrial bioprocess scale-up. Appl Environ Microbiol 81:3288–3298. https://doi.org/10.1128/AEM.00294-15.
51. Ravel B, Newville M. 2005. Athena and Artemis: interactive graphical data analysis using IFEFFIT. Phys Scr 2005:1007. https://doi.org/10.1238/Physica.Topical.115a01007.